Chinese Journal of Aeronautics, (2015), **28(4)**: 1236–1244

Chinese Society of Aeronautics and Astronautics
& Beihang University

Chinese Journal of Aeronautics

cja@buaa.edu.cn
www.sciencedirect.com

Weighted adaptive filtering algorithm for carrier tracking of deep space signal

Song Qingping, Liu Rongke *

School of Electronic and Information Engineering, Beihang University, Beijing 100191, China

Received 22 September 2014; revised 18 December 2014; accepted 29 January 2015
Available online 14 May 2015

KEYWORDS

Adaptive algorithms;
Carrier tracking;
Deep space communication;
Kalman filters;
Tracking accuracy;
Weighted

Abstract Carrier tracking is laid great emphasis and is the difficulty of signal processing in deep space communication system. For the autonomous radio receiving system in deep space, the tracking of the received signal is automatic when the signal to noise ratio (SNR) is unknown. If the frequency-locked loop (FLL) or the phase-locked loop (PLL) with fixed loop bandwidth, or Kalman filter with fixed noise variance is adopted, the accretion of estimation error and filter divergence may be caused. Therefore, the Kalman filter algorithm with adaptive capability is adopted to suppress filter divergence. Through analyzing the inadequacies of Sage–Husa adaptive filtering algorithm, this paper introduces a weighted adaptive filtering algorithm for autonomous radio. The introduced algorithm may resolve the defect of Sage–Husa adaptive filtering algorithm that the noise covariance matrix is negative definite in filtering process. In addition, the upper diagonal (UD) factorization and innovation adaptive control are used to reduce model estimation errors, suppress filter divergence and improve filtering accuracy. The simulation results indicate that compared with the Sage–Husa adaptive filtering algorithm, this algorithm has better capability to adapt to the loop, convergence performance and tracking accuracy, which contributes to the effective and accurate carrier tracking in low SNR environment, showing a better application prospect.

1. Introduction

The exploration to Mars and even deeper space has great significance for solving resource shortage problem faced by humanity and revealing the origin of life, etc. Telemetry, tracking and control (TT&C) technology is the dominant factor in the success of deep space exploration. The biggest challenge for the deep space TT&C is that the received signal is extremely weak due to the long communication distance. Hence, it is difficult for normal carrier tracking to obtain the status and telemetry information of the deep space detector. Given all this, the study on the carrier tracking algorithm of the receiving systems with extremely low signal to noise ratio (SNR) has become the key issue for deep space TT&C. The conventional deep space TT&C receivers implement carrier tracking through frequency-locked loop (FLL) or phase-locked loop (PLL) so as to realize carrier synchronization.[1,2] When the SNR is low, the signal is deeply buried in noise,

* Corresponding author. Tel.: +86 10 82339475.
E-mail address: rongke_liu@buaa.edu.cn (R. Liu).
Peer review under responsibility of Editorial Committee of CJA.

ELSEVIER Production and hosting by Elsevier

http://dx.doi.org/10.1016/j.cja.2015.05.001
1000-9361

which brings great difficulty to the carrier tracking of signal. In order to track the signal stably, usually it decreases the bandwidth of the loop filter. However, when the Doppler shift of the signal is relatively large, the method of reducing bandwidth can not guarantee correct carrier tracking because the Doppler shift may be larger than the capture range. The Kalman filter (KF)[3] or extended Kalman filter (EKF)[4] is considered to be able to break the limitations of bandwidth. In Ref.[5–7], the closed loop KF algorithm was proposed. The closed loop KF algorithms consider the output of phase discriminator or frequency discriminator as the observation variables of KF instead of loop filter so as to break the limitations of loop bandwidth. Also, in Ref.[8,9], EKF was adopted to estimate the frequency directly based on open loop, with a simple structure and low complexity. In Ref.[10], the Doppler frequency estimated by EKF was injected into local oscillator to remove the dynamics from the received signal, which can reduce the loop bandwidth and improve the tracking accuracy.

In Ref.[3–10], it was supposed that the SNR of the received signal was accurately known. Nevertheless, in deep space, an orbiter may communicate with landers in different systems, in which case the transmit power, environment temperature, received circuit parameters and antenna angle errors of the spacecraft are usually unknown, and the receiving system has to track the signal without knowing the SNR. Furthermore, the output noise from the discriminator (phase discriminator or frequency discriminator) is not equivalent to the original observation noise because of the nonlinear effect of the discriminator. Especially if the random phase jitter exists, it will be even harder to get the accurate noise statistic properties. In consideration of these defects, the common Kalman filter in Ref.[3–10] should not be the best choice for filter tracking in low carrier to noise ratio (CNR) conditions due to lower estimation accuracy and filter divergence. To cope with the problem, the autonomous radio technology should be adopted in receiving signal automatically without prior information about SNR characteristics. An autonomous radio system usually adopts the adaptive Kalman filtering (AKF) algorithm to track the carrier signal. For example, in Ref.[11], the adaptive robust Kalman filter was adopted to regulate the filtering gain by introducing an adaptive factor. Also, in Ref.[12], an adaptive factor was introduced to regulate the error covariance matrix. However, in Ref.[11,12] only the dynamic model errors were resisted and the noise variance matrixes could not be adjusted adaptively according to the current SNR environment. In addition, in Ref.[13,14] the AKF algorithm based on maximum likelihood estimation was introduced to estimate process noise covariance and measure noise covariance according to actual conditions, but the computation amount was too large to realize. Meanwhile, it had poor adaptability to unknown noise environment owing to the maximum likelihood estimation based on a piece of data, therefore it would take a long time to track the received signal. In Ref.[15], the algorithm determined the measurement noise covariance based on SNR estimation, and then adjusted the equivalent loop noise bandwidth adaptively according to actual noise power. Compared with the PLL with fixed loop bandwidth, this algorithm has a more favorable carrier phase estimation precision, which can operate when the CNR is 25 dB-Hz. However, if the CNR is less than 30 dB-Hz, the estimation error will increase sharply. Compared with other algorithms, the Sage–Husa adaptive filter algorithm mentioned in Ref.[16–18] has been used more widely. With the features of simple calculation and good real-time, it can utilize the observation value to correct the predicted value in the filtering process and simultaneously estimate and correct unknown noise statistics parameters. However, in the practice of carrier tracking, as the noise covariance matrix of Sage–Husa filter may not be positive semi-definite or positive definite, great errors may be generated in the filtering gain, which will affect the precision of the frequency estimation and even lead to filter divergence.

Considering the drawbacks of the existing algorithms, this paper presents a weighted AKF algorithm, which constructs weighting functions according to the filtering convergence conditions to improve the method of determining the noise covariance matrix of Sage–Husa algorithm and solve the problem that the noise covariance matrix may be negative definite. Besides, UD factorization and adaptive filter are combined in this paper. The innovation adaptive control is also introduced to correct the innovations in filtering process so as to improve the filtering accuracy. The simulation results prove that the tracking accuracy of the algorithm proposed in this paper is better than that of Sage–Husa adaptive filtering algorithm. Moreover, the loss of tracking accuracy of this algorithm is less than that of Sage–Husa algorithm and common Kalman filter algorithm when the phase noise exists.

The content of this paper is arranged as follows. Section 2 provides the carrier tracking loop structure based on AKF and the system model. Section 3 describes the Sage–Husa adaptive filtering algorithm. Section 4 presents the weighted adaptive Kalman filtering algorithm. Section 5 presents the simulation results and performance analysis. Finally, major conclusions are drawn in Section 6.

2. Carrier tracking loop structure

Unlike conventional carrier tracking loops, the frequency update of local numerically controlled oscillator (NCO) in the carrier tracking loop based on AKF is the output of AKF algorithm. The schematic diagram of the carrier tracking loop based on AKF is shown in Fig. 1.

As shown in Fig. 1, the phase difference between actual carrier and local carrier is put into AKF as the observation value. Then the AKF adjusts the frequency of the local carrier from the output in order to make the carrier tracking loop locked. The state vector to be estimated is $\boldsymbol{X}_k = [\,x_{\Delta\varphi} \quad x_{\Delta\omega} \quad x_{\Delta a}\,]^{\mathrm{T}}$, which is the output of AKF algorithm, where $x_{\Delta\varphi}$ is the phase difference between actual carrier and local carrier, $x_{\Delta\omega}$ Doppler frequency shift, and $x_{\Delta a}$ Doppler changing rate. Then the following state equation of the system can be obtained:

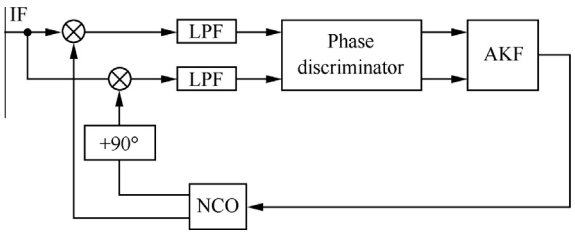

Fig. 1 Carrier tracking loop based on AKF.

$$\boldsymbol{X}_{k+1} = \boldsymbol{\Phi}\boldsymbol{X}_k + \boldsymbol{w}_k = \begin{bmatrix} 1 & T_s & T_s^2/2 \\ 0 & 1 & T_s \\ 0 & 0 & 1 \end{bmatrix} \begin{bmatrix} x_{\Delta\varphi} \\ x_{\Delta\omega} \\ x_{\Delta a} \end{bmatrix}_k + \begin{bmatrix} w_1 \\ w_2 \\ w_3 \end{bmatrix}_k \quad (1)$$

where $\boldsymbol{\Phi}$ is the state transition matrix, T_s the sample interval, and $\boldsymbol{w}_k$ state noise vector with covariance $\boldsymbol{Q}_k$.

The observation equation can be expressed as follows:

$$\boldsymbol{z}_k = \boldsymbol{H}_k\boldsymbol{X}_k + \boldsymbol{n}_k = \left[1, \frac{T_s}{2}, \frac{T_s^2}{6}\right] \begin{bmatrix} x_{\Delta\varphi} \\ x_{\Delta\omega} \\ x_{\Delta a} \end{bmatrix}_k + \boldsymbol{n}_k \quad (2)$$

where $\boldsymbol{z}_k$ is the observation value calculated by phase discriminator during each sampling interval, $\boldsymbol{H}_k$ the system observation matrix and $\boldsymbol{n}_k$ the Gaussian white noise vector for observation. The covariance matrix of $\boldsymbol{n}_k$ is $\boldsymbol{R}_k$.

3. Sage–Husa adaptive filtering algorithm

Sage–Husa adaptive filter algorithm, also known as maximum a posterior (MAP) estimator, estimates recursively using measured data. This algorithm can estimate and modify statistical properties of system noise and measuring noise, thus decreasing model errors, suppressing filter divergence and improving filtering accuracy. The Sage–Husa adaptive filtering algorithm can be described as[16]

$$\hat{\boldsymbol{X}}_{k|k-1} = \boldsymbol{\Phi}\hat{\boldsymbol{X}}_{k-1} + \hat{\boldsymbol{q}}_{k-1} \quad (3)$$

$$\boldsymbol{P}_{k|k-1} = \boldsymbol{\Phi}\boldsymbol{P}_{k-1}\boldsymbol{\Phi}^{\mathrm{T}} + \hat{\boldsymbol{Q}}_k \quad (4)$$

$$\boldsymbol{K}_k = \boldsymbol{P}_{k|k-1}\boldsymbol{H}_k^{\mathrm{T}}\left(\boldsymbol{H}_k\boldsymbol{P}_{k|k-1}\boldsymbol{H}_k^{\mathrm{T}} + \hat{\boldsymbol{R}}_k\right)^{-1} \quad (5)$$

$$\hat{\boldsymbol{X}}_k = \hat{\boldsymbol{X}}_{k|k-1} + \boldsymbol{K}_k\left(\boldsymbol{z}_k - \boldsymbol{H}_k\hat{\boldsymbol{X}}_{k|k-1} - \hat{\boldsymbol{r}}_k\right) \quad (6)$$

$$\boldsymbol{P}_k = (\boldsymbol{I} - \boldsymbol{K}_k\boldsymbol{H}_k)\boldsymbol{P}_{k|k-1} \quad (7)$$

where $\hat{\boldsymbol{X}}_k$ is the estimated value of $\boldsymbol{X}_k$, $\hat{\boldsymbol{X}}_{k|k-1}$ predicted value of $\boldsymbol{X}_k$, $\boldsymbol{P}_k$ the estimated error covariance matrix of $\boldsymbol{X}_k$, $\boldsymbol{P}_{k|k-1}$ the predicted error covariance matrix of $\boldsymbol{X}_k$, $\hat{\boldsymbol{q}}_k$ the estimated mean value of $\boldsymbol{w}_k$, $\hat{\boldsymbol{r}}_k$ the estimated mean value of $\boldsymbol{n}_k$ and $\boldsymbol{K}_k$ Kalman filtering gain. Then, $\hat{\boldsymbol{q}}_k$, $\hat{\boldsymbol{Q}}_k$, $\hat{\boldsymbol{r}}_k$ and $\hat{\boldsymbol{R}}_k$ can be iterated from the time-varying noise estimator as follows:

$$\hat{\boldsymbol{q}}_k = (1 - d_k)\hat{\boldsymbol{q}}_{k-1} + d_k\left(\hat{\boldsymbol{X}}_k - \boldsymbol{\Phi}\hat{\boldsymbol{X}}_{k-1}\right) \quad (8)$$

$$\hat{\boldsymbol{Q}}_k = (1 - d_k)\hat{\boldsymbol{Q}}_{k-1} + d_k\left(\boldsymbol{K}_k\boldsymbol{e}_k\boldsymbol{e}_k^{\mathrm{T}}\boldsymbol{K}_k^{\mathrm{T}} + \boldsymbol{P}_k - \boldsymbol{\Phi}\boldsymbol{P}_{k-1}\boldsymbol{\Phi}^{T}\right) \quad (9)$$

$$\hat{\boldsymbol{r}}_k = (1 - d_k)\hat{\boldsymbol{r}}_{k-1} + d_k\left(\boldsymbol{z}_k - \boldsymbol{H}_k\hat{\boldsymbol{X}}_{k|k-1}\right) \quad (10)$$

$$\hat{\boldsymbol{R}}_k = (1 - d_k)\hat{\boldsymbol{R}}_{k-1} + d_k\left(\boldsymbol{e}_k\boldsymbol{e}_k^{\mathrm{T}} - \boldsymbol{H}_k\boldsymbol{P}_{k|k-1}\boldsymbol{H}_k^{\mathrm{T}}\right) \quad (11)$$

where $d_k = (1 - b)/\left(1 - b^{k+1}\right)$, $\boldsymbol{e}_k$ is the innovation and b is forgetting factor $(0 < b < 1)$. As shown in Eqs. (3)–(11), the statistical calculation of system noise is intensified in the Sage–Husa adaptive Kalman filter algorithm compared with the classic Kalman filter. The forgetting factor is introduced to control the observation weight at different times. The effect of the previous observation is diminished while that of the present observation is enhanced during the filter processing.

4. Weighted adaptive Kalman filtering algorithm

4.1. Determination of noise covariance matrix

As shown in Eqs. (9) and (11), the positive definiteness or positive semi-definiteness of the noise covariance matrix $\hat{\boldsymbol{Q}}_k$ and $\hat{\boldsymbol{R}}_k$ can not be guaranteed because of the minus in those calculation formulas. As can be seen from Eqs. (4) and (5), the non-positive definiteness of $\hat{\boldsymbol{Q}}_k$ may lead $\boldsymbol{P}_{k|k-1}$ to be non-positive definite.[13] And, the non-positive definiteness of $\boldsymbol{P}_{k|k-1}$ or $\hat{\boldsymbol{R}}_k$ may lead $\boldsymbol{H}_k\boldsymbol{P}_{k|k-1}\boldsymbol{H}_k^{\mathrm{T}} + \hat{\boldsymbol{R}}_k$ to be a singular matrix or mostly singular matrix. Therefore, the inverse matrix of $\boldsymbol{H}_k\boldsymbol{P}_{k|k-1}\boldsymbol{H}_k^{\mathrm{T}} + \hat{\boldsymbol{R}}_k$ does not exist or has a great error, which causes a great estimation error of $\boldsymbol{K}_k$ and $\hat{\boldsymbol{X}}_k$, even leads to filter divergence.

In order to ensure the positive semi-definiteness of the process noise covariance matrix $\hat{\boldsymbol{Q}}_k$, the changes of the estimation error covariance matrix $\boldsymbol{P}_k$ should be negligible. Thus, the following iterative form of $\hat{\boldsymbol{Q}}_k$ is obtained:[13]

$$\hat{\boldsymbol{Q}}_k = (1 - d_k)\hat{\boldsymbol{Q}}_{k-1} + d_k\left(\boldsymbol{K}_k\boldsymbol{e}_k\boldsymbol{e}_k^{\mathrm{T}}\boldsymbol{K}_k^{\mathrm{T}}\right) \quad (12)$$

The observation noise covariance matrix $\hat{\boldsymbol{R}}_k$ can be improved according to the filtering convergence conditions, which is judged by the innovation $\boldsymbol{e}_k$. The innovation $\boldsymbol{e}_k$ in filtering process is defined as the difference of the observation value $\boldsymbol{z}_k$ and the predicted observation value $\hat{\boldsymbol{z}}_{k|k-1}$, which is expressed as follows:

$$\boldsymbol{e}_k = \boldsymbol{z}_k - \hat{\boldsymbol{z}}_{k|k-1} = \boldsymbol{H}_k\boldsymbol{X}_k + \boldsymbol{n}_k - \boldsymbol{H}_k\hat{\boldsymbol{X}}_{k|k-1} = \boldsymbol{H}_k\tilde{\boldsymbol{X}}_{k|k-1} + \boldsymbol{n}_k \quad (13)$$

where $\tilde{\boldsymbol{X}}_{k|k-1} = \boldsymbol{X}_k - \hat{\boldsymbol{X}}_{k|k-1}$ is predicted error. The theoretical mean value of $\boldsymbol{e}_k$ is described as

$$E(\boldsymbol{e}_k) = \boldsymbol{H}_k E\left(\tilde{\boldsymbol{X}}_{k|k-1}\right) + E(\boldsymbol{n}_k) = 0 \quad (14)$$

According to $\boldsymbol{P}_{k|k-1} = E\left(\tilde{\boldsymbol{X}}_{k|k-1}\tilde{\boldsymbol{X}}_{k|k-1}^{\mathrm{T}}\right)$ and $\hat{\boldsymbol{R}}_k = E\left(\boldsymbol{n}_k\boldsymbol{n}_k^{\mathrm{T}}\right)$, the theoretical variance value of estimation error is written as

$$\begin{aligned} \boldsymbol{S}_k &= E\left(\boldsymbol{e}_k\boldsymbol{e}_k^{\mathrm{T}}\right) = E\left[\left(\boldsymbol{H}_k\tilde{\boldsymbol{X}}_{k|k-1} + \boldsymbol{n}_k\right)\left(\boldsymbol{H}_k\tilde{\boldsymbol{X}}_{k|k-1} + \boldsymbol{n}_k\right)^{\mathrm{T}}\right] \\ &= \boldsymbol{H}_k\boldsymbol{P}_{k|k-1}\boldsymbol{H}_k^{\mathrm{T}} + \hat{\boldsymbol{R}}_k \end{aligned} \quad (15)$$

where $\boldsymbol{S}_k$ is also named as average estimation error in the filtering process. As $\boldsymbol{e}_k^{\mathrm{T}}\boldsymbol{e}_k$ is the actual filter estimation error, innovation $\boldsymbol{e}_k$ could be used to judge the filtering convergence. The filtering convergence criterion can be concluded by Ref.[19]:

$$\boldsymbol{e}_k^T\boldsymbol{e}_k \leqslant \gamma \mathrm{tr}\left(E\left(\boldsymbol{e}_k\boldsymbol{e}_k^{\mathrm{T}}\right)\right) \quad (16)$$

where tr is the trace of the matrix and γ a variable coefficient with $\gamma \geqslant 1$. $\gamma = 1$ is the most strict condition for convergence judgment. The filtering convergence can be concluded when Eq. (16) is equal. Otherwise, the actual filter error is higher than γ times of the value of the theoretical variance, indicating that the current observation noise variance estimation is lower than actual value. To correct noise covariance matrix $\hat{\boldsymbol{R}}_k$ according to the actual SNR environment, a weighted exponential function $f_k(v_k)$ is proposed, which is expressed as follows:

$$f_k(v_k) = \lambda^{v_k - 1} \tag{17}$$

$$v_k = \left(\boldsymbol{e}_k^{\mathrm{T}} \boldsymbol{e}_k\right) / \gamma \mathrm{tr}\left(E\left(\boldsymbol{e}_k \boldsymbol{e}_k^{\mathrm{T}}\right)\right) \tag{18}$$

where $1 < \lambda < 2$ and $\gamma = 1$ are satisfied. In addition, $\hat{\boldsymbol{R}}_k$ is calculated as follows:

$$\hat{\boldsymbol{R}}_k = f_k(v_k) \hat{\boldsymbol{R}}_{k-1} \tag{19}$$

The exponential function $f_k(v_k)$ includes the following properties:

(1) $f_k(v_k)$ is monotone, continuous and differentiable.
(2) When $v_k \in (-\infty, +\infty)$, $f_k(v_k) > 0$ is satisfied.

According to the nature of the exponential function, if v_k is higher than 1, $f_k(v_k) > 1$, then $\hat{\boldsymbol{R}}_k$ must be increased; otherwise, if v_k is lower than 1, $f_k(v_k) < 1$, $\hat{\boldsymbol{R}}_k$ must be decreased. Therefore, the value of $\hat{\boldsymbol{R}}_k$ can be adjusted adaptively according to the actual SNR environment. When $f_k(v_k) = 1$, the adaptive filtering algorithm becomes common Kalman filtering algorithm.

The initial value of $\hat{\boldsymbol{R}}_k$ can be determined by

$$\hat{\boldsymbol{R}}_k = \sigma^2 \boldsymbol{I} \tag{20}$$

where σ^2 is the observation noise variance and $\boldsymbol{I}$ an unit matrix. If ρ represents the signal to noise ratio (Unit: dB) and A is the signal amplitude, then the following expression of σ^2 is obtained:

$$\sigma^2 = 10^{\wedge}\left[\left(10 \lg \frac{A^2}{2} - \rho\right) / 10\right] \tag{21}$$

From Eq. (21), we can see $\sigma^2 > 0$, which leads the initial matrix of $\hat{\boldsymbol{R}}_k$ to be positive definite. As is known that the properties of the exponential function, $f_k(v_k) > 0$. Therefore, $\hat{\boldsymbol{R}}_k$ can be adjusted adaptively and remain positive definite during the filtering process, which improves the convergence performance of the filter significantly. As the equivalent noise bandwidth of the carrier tracking loop is directly proportional to $\hat{\boldsymbol{Q}}_k / \hat{\boldsymbol{R}}_k$,[15] after adaptive adjustment of $\hat{\boldsymbol{Q}}_k$ and $\hat{\boldsymbol{R}}_k$ based on Eqs. (12) and (19), the optimal equivalent noise bandwidth can be obtained according to actual SNR environment.

4.2. Error covariance matrix determined by UD factorization

In practice, even if both $\hat{\boldsymbol{Q}}_k$ and $\hat{\boldsymbol{R}}_k$ are positive definite, it is still very difficult to guarantee the positive definiteness of the error covariance matrix in view of the accumulation of rounding errors. Therefore, UD factorization algorithm is put forward in this paper to guarantee the non-negative definiteness of the error covariance matrix. UD factorization decomposes the error covariance matrix into the form of $\boldsymbol{U}\boldsymbol{D}\boldsymbol{U}^T$, where $\boldsymbol{U}$ is an upper triangular matrix whose main diagonal elements are 1 and $\boldsymbol{D}$ is a diagonal matrix.

$\boldsymbol{U}$ and $\boldsymbol{D}$ are updated in each filtering period. The procedures of UD factorization algorithm are divided into the measurement update stage and time update stage in which the solution results are determined by $\boldsymbol{\Phi}$, $\boldsymbol{H}_k$, $\hat{\boldsymbol{Q}}_k$, $\hat{\boldsymbol{R}}_k$ as well as $\boldsymbol{U}$ and $\boldsymbol{D}$ in the previous filtering period.[20] In each filtering period, $\boldsymbol{P}_{k|k-1}$ is factorized into the following form:

$$\boldsymbol{P}_{k|k-1} = \boldsymbol{U}\boldsymbol{D}\boldsymbol{U}^{\mathrm{T}} \tag{22}$$

Putting Eq. (22) into Eq. (15), the following theoretical value of innovation variance is obtained:

$$\boldsymbol{S}_k = \boldsymbol{H}_k \boldsymbol{U}\boldsymbol{D}\boldsymbol{U}^T \boldsymbol{H}_k^{\mathrm{T}} + \hat{\boldsymbol{R}}_k \tag{23}$$

When $\boldsymbol{F} = \boldsymbol{D}\boldsymbol{G}$ and $\boldsymbol{G} = (\boldsymbol{H}_k U)^{\mathrm{T}}$, the filtering gain matrix $\boldsymbol{K}_k$ is

$$\boldsymbol{K}_k = \boldsymbol{U}\boldsymbol{F}\boldsymbol{S}_k^{-1} \tag{24}$$

Substituting both Eqs. (22) and (24) into Eq. (7), the $\boldsymbol{P}_k$ is obtained as follows:

$$\begin{aligned} \boldsymbol{P}_k &= \boldsymbol{P}_{k|k-1} - \boldsymbol{K}\boldsymbol{H}_k \boldsymbol{P}_{k|k-1} = \boldsymbol{U}\boldsymbol{D}\boldsymbol{U}^{\mathrm{T}} - \boldsymbol{U}\boldsymbol{F}\boldsymbol{S}_k^{-1} \boldsymbol{H}_k \boldsymbol{U}\boldsymbol{D}\boldsymbol{U}^{\mathrm{T}} \\ &= \boldsymbol{U}\left(\boldsymbol{D} - \boldsymbol{F}\boldsymbol{S}_k^{-1} \boldsymbol{F}^T\right) \boldsymbol{U}^T \end{aligned} \tag{25}$$

According to Eqs. (22) and (25), $\boldsymbol{U}$ and $\boldsymbol{D}$ are solved to calculate $\boldsymbol{P}_{k|k-1}$ and $\boldsymbol{P}_k$ during the UD factorization process instead of calculating $\boldsymbol{P}_{k|k-1}$ and $\boldsymbol{P}_k$ directly. The non-negative definiteness of the error covariance matrix is guaranteed by the special structure of $\boldsymbol{U}$ and $\boldsymbol{D}$ and the non-negative definiteness of $\hat{\boldsymbol{R}}_k$ and $\hat{\boldsymbol{Q}}_k$.

The algorithm developed in this paper combines the UD factorization and the adaptive filtering to determine the noise variance matrix $\hat{\boldsymbol{Q}}_k$ and $\hat{\boldsymbol{R}}_k$ to get the solutions of $\boldsymbol{U}$ and $\boldsymbol{D}$. It has been shown that the algorithm cannot only estimate and correct the statistics properties of the process noise and the observation noise in real time, but also overcome the poor stability of the error covariance matrix during the filtering process, so it can improve filtering accuracy and ensure the convergence distinctly.

4.3. Correct outliers based on an innovation adaptive control

Under low SNR conditions in deep space, noise obviously affects observations, potentially leading to abnormal observations that exceed the acceptable range. The innovation errors increase because of abnormal observations; thus, normal filtering is disturbed. An abnormal observation at time k can be expressed as follows:

$$\boldsymbol{z}_k' = \boldsymbol{z}_k + \boldsymbol{B} \tag{26}$$

where $\boldsymbol{z}_k'$ is an abnormal observation, and $\boldsymbol{B}$ is an offset that is added to the normal observation. Therefore, an abnormal innovation $\boldsymbol{e}_k'$ can be expressed as follows:

$$\boldsymbol{e}_k' = \boldsymbol{z}_k' - \boldsymbol{H}_k \hat{\boldsymbol{X}}_{k|k-1} - \hat{\boldsymbol{r}}_k = \boldsymbol{z}_k + \boldsymbol{B} - \boldsymbol{H}_k \hat{\boldsymbol{X}}_{k|k-1} - \hat{\boldsymbol{r}}_k = \boldsymbol{e}_k + \boldsymbol{B} \tag{27}$$

According to Eq. (27), when the observation value becomes abnormal, the properties of the innovation series deviate the normal statistical properties. Therefore, the relationship between the innovation series and the filtering estimated value can be expressed as follows:

$$\begin{aligned} \hat{\boldsymbol{X}}_k &= \hat{\boldsymbol{X}}_{k|k-1} + \boldsymbol{K}_k \boldsymbol{e}_k = \boldsymbol{\Phi}\hat{\boldsymbol{X}}_{k-1} + \boldsymbol{K}_k \boldsymbol{e}_k \\ &= \boldsymbol{\Phi}\left(\boldsymbol{\Phi}\hat{\boldsymbol{X}}_{k-2} + \boldsymbol{K}_{k-1}\boldsymbol{e}_{k-1}\right) + \boldsymbol{K}_k \boldsymbol{e}_k \\ &= \boldsymbol{\Phi}^2 \hat{\boldsymbol{X}}_{k-2} + \boldsymbol{\Phi}\boldsymbol{K}_{k-1}\boldsymbol{e}_{k-1} + \boldsymbol{K}_k \boldsymbol{e}_k \\ &= \boldsymbol{\Phi}^n \hat{\boldsymbol{X}}_{k-n} + \boldsymbol{\Phi}^{n-1} \boldsymbol{K}_{k-n+1} \boldsymbol{e}_{k-n+1} + \ldots + \boldsymbol{\Phi}\boldsymbol{K}_{k-1}\boldsymbol{e}_{k-1} + \boldsymbol{K}_k \boldsymbol{e}_k \end{aligned} \tag{28}$$

According to Eq. (28), the filtering estimated value is a linear combination of the innovation series. The abnormal innovations induced by the abnormal observation cannot

correct predicted value accurately. Hence, if the innovations are not pretreated, the errors of the filtering estimated value would accumulate when the abnormal innovations appear continually, the errors increase continually, and the reliability of the filter is thus reduced, which may lead to filter divergence. However, because the Sage–Husa algorithm lacks a disposal of the abnormal innovations, we developed a new method based on innovation adaptive control for detecting and correcting the filter innovation $\boldsymbol{e}_k$ in real time during the filtering process to correct the outliers. Even for large-error situations, the effects of abnormal innovations on the filtering estimated value can be diminished and confined to a preset range by adaptive control to ensure that the filtering estimated value is as close as possible to the actual state of the system.

To realize the innovation adaptive control, $\boldsymbol{e}_k$ can be replaced by $g_k\boldsymbol{e}_k$, where g_k is a smooth weighted function. The filtering estimated value is thus expressed as follows:

$$\hat{\boldsymbol{X}}_k^c = \hat{\boldsymbol{X}}_{k|k-1} + \boldsymbol{K}_k g_k \boldsymbol{e}_k \tag{29}$$

where $\hat{\boldsymbol{X}}_k^c$ is the estimated value corrected using a weighting function. This paper presents an algorithm based on the filtering convergence criterion for determining g_k. According to Eq. (16) and the cut-off of functions, a set of weighting functions can be formed:

$$S = \{g_k(v_k) | g_k(v_k) \leqslant 1, g_k(v_k) \leqslant 1/v_k,\ v_k \in [0, +\infty)\} \tag{30}$$

where the definition of v_k is the same as that shown in Eq. (18), and the variable coefficient γ is equal to 1. If a Kalman filter is convergent, then v_k is lower than 1, indicating that the innovations are normal without inducing changes. Otherwise, if the Kalman filter is divergent, then v_k is higher than 1, indicating that the innovations may be abnormal and should be corrected by the factor $1/v_k$. To minimize the mean square error of the filtering estimated value, the optimization model can be established as follows:

$$\min_S \left\{ E\left(\left\| \hat{\boldsymbol{X}}_k^c - \hat{\boldsymbol{X}}_{k|k-1} \right\|^2 \right) \right\} \tag{31}$$

The expansion of $E\left(\left\| \hat{\boldsymbol{X}}_k^c - \hat{\boldsymbol{X}}_{k|k-1} \right\|^2 \right)$ after simplification is expressed as follows:

$$\begin{aligned} E\left(\left\| \hat{\boldsymbol{X}}_k^c - \hat{\boldsymbol{X}}_{k|k-1} \right\|^2 \right) &= E\left(\left\| \hat{\boldsymbol{X}}_k^c - \hat{\boldsymbol{X}}_k + \hat{\boldsymbol{X}}_k - \hat{\boldsymbol{X}}_{k|k-1} \right\| \right) \\ &= E\left(\left\| \hat{\boldsymbol{X}}_k^c - \hat{\boldsymbol{X}}_k \right\|^2 \right) + E\left(\left\| \hat{\boldsymbol{X}}_k - \hat{\boldsymbol{X}}_{k|k-1} \right\|^2 \right) \\ &\quad + 2E\left(\hat{\boldsymbol{X}}_k^c - \hat{\boldsymbol{X}}_k \right)^{\mathrm{T}} \left(\hat{\boldsymbol{X}}_k^c - \hat{\boldsymbol{X}}_k \right) \\ &= E\left(\left\| \hat{\boldsymbol{X}}_k^c - \hat{\boldsymbol{X}}_k \right\|^2 \right) + E\left(\left\| \hat{\boldsymbol{X}}_k - \hat{\boldsymbol{X}}_{k|k-1} \right\|^2 \right) \end{aligned} \tag{32}$$

According to Eq. (32), the problem is transformed to solve the minimum of $E\left(\left\| \hat{\boldsymbol{X}}_k^c - \hat{\boldsymbol{X}}_k \right\|^2 \right)$ in set S. According to the definitions of $\hat{\boldsymbol{X}}_k^c$ and $\hat{\boldsymbol{X}}_k$, $E\left(\left\| \hat{\boldsymbol{X}}_k^c - \hat{\boldsymbol{X}}_k \right\|^2 \right)$ can be expressed as follows:

$$E\left(\left\| \hat{\boldsymbol{X}}_k^c - \hat{\boldsymbol{X}}_k \right\|^2 \right) = E\left\{ [g_k(v_k) - 1]^2 \left\| K_k \boldsymbol{e}_k \right\|^2 \right\} \tag{33}$$

According to the definition of set S, the minimum of $E\left(\left\| \hat{\boldsymbol{X}}_k^c - \hat{\boldsymbol{X}}_k \right\|^2 \right)$ can be derived by setting the innovation control function as follows:

$$g_k(v_k) = \begin{cases} 1 & v_k < 1 \\ 1/v_k & v_k \geqslant 1 \end{cases} \tag{34}$$

The properties of $g_k(v_k)$ are outlined as follows:

(1) $g_k(v_k)$ is monotonous, continuous and differentiable.
(2) When $v_k \to \infty$, $g_k(v_k) \to 0$ is satisfied.
(3) $g_k(v_k)$ has a cut-off property, that is, when $v_k < 1$ or $v_k \geqslant 1$, $g_k(v_k)$ is a constant where 1 is the threshold.

In each filtering period, $g_k(v_k)$ can adjust the innovation continuously and effectively, to correct the abnormal innovations induced by abnormal observations. When the proposed algorithm is used, the filter divergence is avoided to a certain extent and the filtering results are more stable with a higher accuracy compared with those obtained using the Sage–Husa algorithm.

5. Experimental results and performance analysis

The signal frequency used in this study involved the adoption of the constant acceleration model based on the high dynamic motion model of the Jet Propulsion Laboratory. The instantaneous frequency of the received signal is expressed as follows:

$$f_{\mathrm{r}} = f_{\mathrm{i}} + \Delta f + \mathrm{at} \tag{35}$$

where f_{i} is a nominal IF, Δf the Doppler shift, and a the Doppler rate. Because of its high efficiency for power application and satisfactory anti-noise performance, binary phase shift keying (BPSK) modulation has been widely used in deep space communication systems when the SNR is low. The signal source can thus be expressed as follows:

$$y(t) = \mathrm{Ab}(t) \sin\left[2\pi \left(f_{\mathrm{i}} + \Delta f + \frac{1}{2}\mathrm{at} \right) t \right] + n(t) \tag{36}$$

where A is the signal amplitude, $n(t)$ the Gaussian white noise vector, and $b(t)$ the data bit stream with the value of 1 or -1; furthermore, Gaussian noise variance is σ^2 and is expressed in Eq. (21).

The signal model used for the simulations was established according to Eq. (36); the symbol rate was 100 bits per second (bps). A time-domain matching-average periodogram algorithm presented in Ref. [21] was used for capturing the carriers. After the carrier capture, the difference in the Doppler frequency between the local oscillator and the received signal should be lower than 30 Hz, and the Doppler rate should be no higher than 15 Hz/s. Then, the carrier tracking loop based on AKF is turned on.

5.1. Results after adjusting innovation adaptive control

This study performed an innovation adaptive control that detects and corrects the filter innovation $\boldsymbol{e}_k$ in real time during the filtering process. The effects of the errors of the filtering estimated value that are produced by abnormal innovations are diminished by adaptive control, to ensure that the filtering estimated value is as close as possible to the actual state of the system. Fig. 2 shows the modified results of $\boldsymbol{e}_k$ that were obtained using the proposed algorithm when CNR is 24 dB-Hz.

As shown in Fig. 2, before 6 s, the large errors of the abnormal innovations are reduced by adaptive control to improve the filtering accuracy; furthermore, after 6 s, the innovations remain virtually unchanged because the filter is convergent.

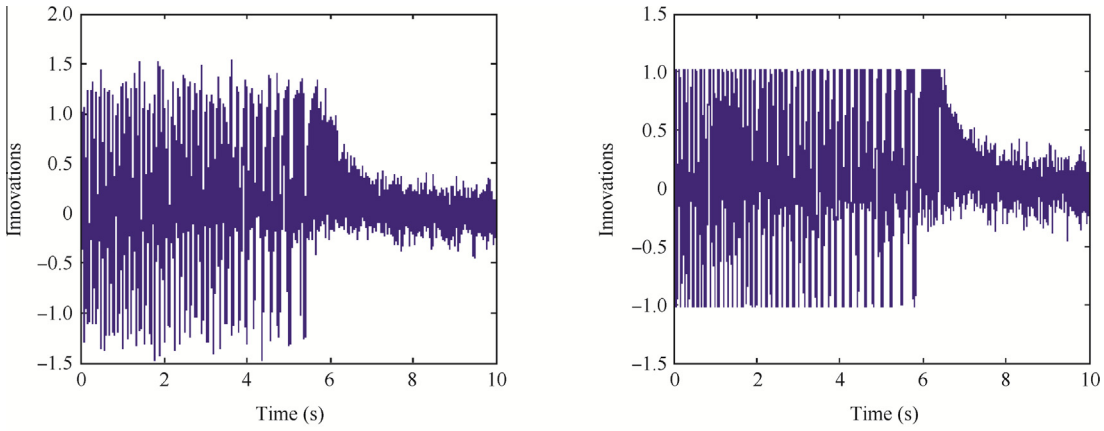

(a) Innovations before correction (b) Innovations after correction

Fig. 2 Innovations of filter.

5.2. Tracking accuracy without phase noise

The bit error rate (BER) performance of the system is extremely sensitive to the offset of the carrier frequency and decreases sharply when the frequency deviation is increased; the received signal is demodulated directly. This is because integrating a frequency offset produces a phase error, which randomly changes the polarity of the data bit and ultimately reduces the BER performance. The relationship between the BER performance of the BPSK modulation and phase error is shown in Eq. (37). The relationship between the phase error and frequency error is expressed in Eq. (38).

$$P = Q\left(\sqrt{(2E_b/N_0)\cdot\cos^2\phi_e}\right) \tag{37}$$

$$\phi_e = \int_0^T \Delta f' \mathrm{d}f \tag{38}$$

where E_b/N_0 is the energy per bit to noise power spectral density ratio, ϕ_e is the phase error, $\Delta f'$ the frequency error, T is one symbol period, and P is BER. As shown in Eqs. (37) and (38), before the demodulation, the BER performance must be improved by increasing the accuracy of the carrier frequency tracking. When the symbol rate is lower, T is higher and the BER performance deteriorates. Therefore, the frequency tracking accuracy must be improved, particularly when the symbol rate is low.

The frequency tracking accuracy is expressed by root mean square (RMS) frequency error. The simulation was executed using the proposed algorithm based on the loop design illustrated in Fig. 1. First, the noise variance is assumed to be known; however, the non-linear effect of the discriminator exists. When the CNR is in the range of 24–33 dB-Hz, the RMS frequency error is obtained through simulation. Fig. 3(a) depicts the RMS frequency errors for a common Kalman filter, Sage–Husa adaptive filter, and the proposed filter, separately.

The results shown in Fig. 3(a) prove that the frequency error of the weighted adaptive filter algorithm is smaller than those of the common Kalman filter and Sage–Husa adaptive filter. Therefore, the proposed filter can solve the non-linear problem of the discriminator to a certain extent.

Second, the noise variance is assumed to be unknown, and the initial measurement noise variance is only one-tenth of the actual value. To test the effects of non-positive definiteness and outliers, the RMS frequency errors for the common Kalman filter, Sage–Husa adaptive filter and noise variance adaptive algorithm in Sections 4.1 and 4.2 without the innovation adaptive control and weighted adaptive filter, respectively, were evaluated. Fig. 3(b) illustrates the resulting RMS frequency errors.

As shown in Fig. 4, an adaptively robust filter algorithm proposed in Ref.[11] is compared with the proposed weighted adaptive filter algorithm when the noise variance is unknown.

Fig. 5 depicts the filter gain variation curves when the CNR is 24 dB-Hz. As shown in this figure, $K(m,n)$ is the element of the mth row and nth column of the filter gain matrix $\boldsymbol{K}_k$.

As illustrated in Figs. 3 and 4, the noise variance matrix of the common Kalman filter cannot be adjusted adaptively in the carrier tracking process, thus resulting in a large estimated value error, particularly in the area with low CNR. When the Kalman filter algorithm with adaptive capability is adopted, the statistical properties of noise variance are modified adaptively to reduce the error of the model estimated value. Furthermore, the frequency error of the weighted adaptive filter algorithm is smaller than that of the Sage–Husa adaptive filter algorithm, adaptively robust filter algorithm and noise variance adaptive algorithm. This is because the Sage–Husa adaptive filter algorithm can not guarantee the positive definiteness of the noise covariance matrix, the noise variance adaptive algorithm lacks disposal to the abnormal innovations, the adaptively robust filter algorithm diminishes only the initial model errors and dynamic errors, and the noise variance matrixes cannot be adjusted adaptively according to the current SNR environment. However, the weighted adaptive filter algorithm improves the methods for determining the noise variance matrix and error covariance matrix and also controls the innovation sequence adaptively.

Fig. 5 shows a further explanation of the phenomenon. The noise variance of the common Kalman filter remains unchanged during the entire estimation process, which requires that the priori information of the system can be obtained more accurately. However, because the initial noise variance is unknown, the gain of the common Kalman filter demonstrates

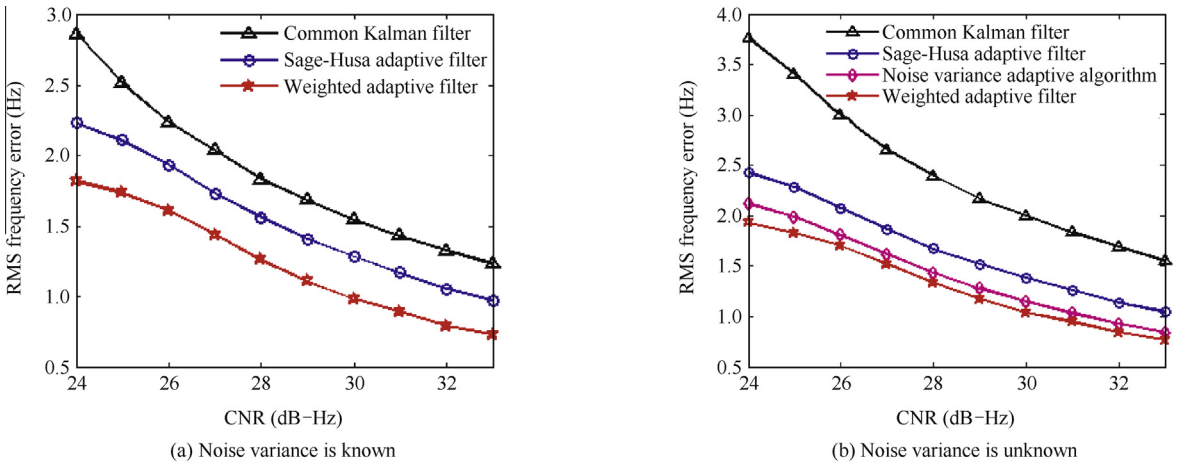

Fig. 3 RMS frequency error.

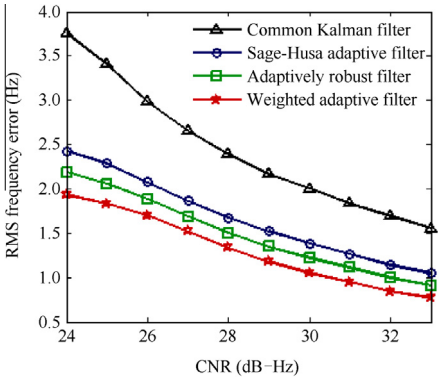

Fig. 4 Comparison of RMS frequency error.

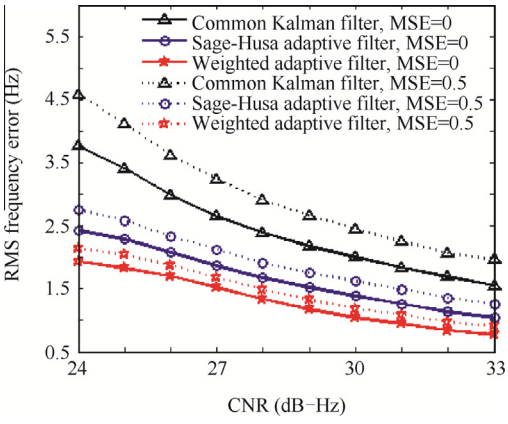

Fig. 6 RMS frequency error with phase noise.

higher error. In addition, the weighted adaptive filter algorithm ensures the positive definiteness of the noise variance matrix and error covariance matrix, and the error of the inverse matrix shown in Eq. (24) is small; thus, $\boldsymbol{K}_k$ is more accurate. When $\boldsymbol{K}_k$ is lower, the effects of observation noise on the filtering estimated value are diminished and the proportion of the predictive value is increased; therefore, the error of the estimated value decreases.

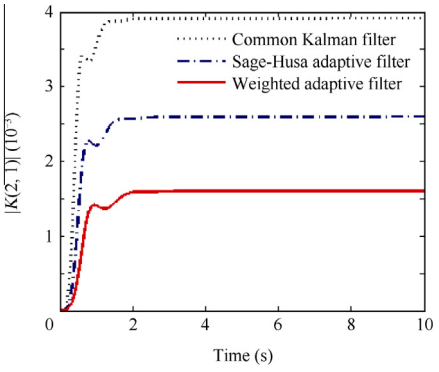

Fig. 5 Curves of filter gain change.

The aforementioned results indicate that the weighted adaptive filter algorithm works efficiently at low CNR. The system state error is reduced effectively and a smaller frequency estimated value error is obtained.

5.3. Tracking accuracy with phase noise

In the actual transmission environment, a phase random jitter exists in both modulation and demodulation systems during the signal transmission because of the phase noise of the local oscillator. Therefore, a signal containing phase noise must be simulated and analyzed. In Ref.[22] a phase random-walk model was studied for simulating the phase noise process, which is expressed as follows:

$$\theta_{\mathrm{pn}} = \theta_{\mathrm{p}} + \Delta_k \tag{39}$$

where θ_{p} is the phase value under normal conditions and without jitter and Δ_k is the noise with a Gaussian distribution $(N(0, \sigma^2))$.When the CNR is in the range of 24–33 dB-Hz, the initial measurement noise variance is only one-tenth of the actual value, the three algorithms discussed in Section 5.2 were used for simulating the received signal with phase noise to obtain the accuracy of the frequency tracking (Fig. 6), where MSE is the mean square error of Δ_k.

As depicted in Fig. 6, the two algorithms with adaptive capability are rarely affected by the phase noise. When the CNR is 24 dB-Hz and MSE is 0.5, the loss of frequency tracking accuracy of both algorithms is lower than 0.3 Hz. Furthermore, the loss of frequency tracking accuracy of the weighted adaptive filter algorithm is slightly lower than that of Sage–Husa algorithm. However, under the same conditions, the loss of frequency tracking accuracy for the common Kalman filter is more than 0.8 Hz. The adaptive filter algorithm has considerable advantages because it estimates and modifies the noise statistical properties continuously according to the phase noise to determine the optimal estimated value.

6. Conclusions

(1) This paper proposes a weighted AKF algorithm for creating a weighting function according to the convergence conditions of Kalman filtering to ensure the non-negative definiteness of the noise covariance matrix, which can realize carrier tracking in an unknown SNR environment.
(2) Furthermore, UD factorization and adaptive filtering are combined in this study to ensure the non-negative definiteness of the error covariance matrix; that is, the algorithm proposed in this paper avoids large errors of filtering estimation and suppresses filter divergence effectively by ensuring the non-negative definiteness of the noise variance matrix and error covariance matrix.
(3) In addition, in this paper, the outliers are corrected using adaptive innovation control created with a weighting function to improve the tracking accuracy. In other words, the abnormal innovations are corrected in real time and the tracking accuracy is improved.
(4) Compared with the common Kalman filtering and Sage–Husa adaptive filtering algorithms, the proposed algorithm achieves higher tracking performance. In particular, regarding phase noise, the proposed algorithm demonstrates the least loss of frequency tracking accuracy; thus, this algorithm is suitable for the autonomous radio receiving system in deep space.

Acknowledgements

This study was supported by Program for New Century Excellent Talents in University of China (No. NCET-12-0030), and National Natural Science Foundation of China (No. 91438116).

References

1. Razavi A, Egziabher DG, Akos DM. Carrier loop architectures for tracking weak GPS signals. *IEEE Trans Aerospace Electron Syst* 2008;**44**(2):697–710.
2. Kazemi PL. Optimum digital filters for GNSS tracking loops*ION GNSS 21st international technical meeting of the satellite division*, 2008 Sep 16–19; Center Savannah, Ga, USA. Manassas, VA: ION; 2008. p. 2304–13.
3. Barreau V, Vigneau W, Macabiau C, Deambrogio L. Kalman filter based robust GNSS signal tracking algorithm in presence of ionospheric scintillations, In: *Satellite navigation technologies and European workshop on GNSS signals and signal processing*, 2012 Dec 5–7; Noordwijk, Holland. Piscataway, NJ: IEEE Press; 2012. p. 1–8.
4. Lashley M, Bevly DM, Hung JY. Performance analysis of vector tracking algorithms for weak GPS signals in high dynamics. *IEEE J Select Topics Signal Process* 2009;**3**(4):661–73.
5. Miao JF, Chen W, Sun YR, Liu JY. Low C/N_0 carrier tracking loop based on optimal estimation algorithm in GPS software receivers. *Chin J Aeronaut* 2010;**23**(1):109–16.
6. Zhang L, Morton Y, Graas FV, Beach T. Characterization of GNSS signal parameters under ionosphere scintillation conditions using software-based tracking algorithms. *Position location and navigation symposium*, 2010 May 4–6; Indian Wells, CA, USA. Piscataway, NJ: IEEE Press; 2010. p. 264–75.
7. Yang YH, Zhou JC, Loffeld O. GPS receiver tracking loop design based on a Kalman filtering approach. *Proceedings of the international symposium ELMAR*, 2012 Sep 12–14; Zadar, Croatia. Piscataway, NJ: IEEE Press; 2012. p. 673–6.
8. Vilnrotter VA, Hinedi S, Kumar R. Frequency estimation techniques for high dynamic trajectories. *IEEE Trans Aerospace Electron Syst* 1989;**25**(4):559–77.
9. Wang SC, Luo DC, Liu ZG, Zhang JS, Zhao X. A hybrid carrier tracking algorithm based on FQFD and EKF. *Asia simulation conference – 7th international conference on system simulation and scientific computing*: 2008 Oct 10–12; Beijing, China. Piscataway, NJ: IEEE Press; 2008. p. 804–8.
10. Li WB, Liu SJ, Zhou CH, Zhou SD, Wang TC. High dynamic carrier tracking using Kalman filter aided phase-lock loop. *International conference on wireless communications, networking and mobile computing*: 2007 Sep 21–25; Shanghai, China. Piscataway, NJ: IEEE Press; 2007. p. 673–6.
11. Miao JF, Chen W, Sun YR, Liu JY. Adaptively robust phase lock loop for low C/N carrier tracking in a GPS software receiver. *Acta Automat Sin* 2011;**37**(1):52–60.
12. Yang YX, Gao WG. An optimal adaptive Kalman filter. *J Geodesy* 2006;**80**(4):177–83.
13. Mohamed AH. *Optimizing the estimation procedure in INS/GPS integration for kinematic applications [dissertation]*. Calgary: University of Calgary; 1999.
14. Papic VD, Djurovic ZM, Kovacevic BD. Adaptive Doppler–Kalman filter for radar systems. *IEE Proc Vision Image Signal Process* 2006;**153**(3):379–87.
15. Won JH, Eissfeller B. A tuning method based on signal-to-noise power ratio for adaptive PLL and its relationship with equivalent noise bandwidth. *IEEE Commun Lett* 2013;**17**(2):393–6.
16. Gao XD, You DY, Katayama S. Seam tracking monitoring based on adaptive Kalman filter embedded elman neural network during high-power fiber laser welding. *IEEE Trans Industr Electron* 2012;**59**(11):4315–25.
17. Pan Y, Song P, Li KJ, Lin R, Huang W. A filtering method of gyroscope random drift for miniature unmanned helicopter. *International conference on computer science and network technology*: 2011 Dec 24–26; Harbin, China. Piscataway, NJ: IEEE Press; 2011. p. 730–4.
18. Cui B, Dong EQ, Li XY, Zhang DJ, Wang JR. A time synchronization algorithm based on bimodal clock frequency estimation. *Asia-pacific conference on communications*, 2012 Oct 15–17; Jeju, Island. Piscataway, NJ: IEEE Press; 2012. p. 75–8.
19. Bi S, Min HQ, Luo B, Li C. An adaptive filtering method to improve measurement accuracy of walking robot attitude. *International conference on cyber technology in automation, control, and intelligent systems;* 2011 Mar 20–23; Kunming, China. Piscataway, NJ: IEEE Press; 2011. p. 67–71.
20. Spingarn K, Robinson BH. Attitude determination with UD implementation of decoupled bias estimation. *IEEE Trans Aerospace Electron Syst* 2007;**43**(4):1294–304.

21. Satorius E, Estabrook P, Wilson J, Fort D. Direct-to-earth communications and signal processing for Mars exploration rover entry, descent, and landing, IPN Progress Report 42-153. Pasadena, California: Jet Propulsion Laboratory; 2003.
22. Valle's EL, Wesel RD, Villasenor JD, Jones CR, Simon M. Pilotless carrier phase- synchronization via LDPC code feedback. *Military communications conference;* 2010 Oct 31–Nov 3; San Jose, CA, USA. Piscataway, NJ: IEEE Press; 2010. p. 2068–73.

Song Qingping is a Ph.D. student at School of Electronic and Information Engineering, Beihang University. He received his B.S. degree from Northwestern Polytechnical University. His main research interest is deep space communication.

Liu Rongke is a professor at School of Electronic and Information Engineering, Beihang University. His area of research includes aerospace communication, wireless multimedia communication, and integrated circuit design.